THERMOLUMINESCENCE AND SCINTILLATION TIME PROFILES OF BaF_2:Ce*

J. GŁODO[a,b†], P. SZUPRYCZYŃSKI[a,b] AND A.J. WOJTOWICZ[b,a]

[a]Chemistry Dept., Boston University
590 Commonwealth Ave., Boston MA 02215, USA
[b]Institute of Physics, N. Copernicus University
Grudziądzka 5/7, 87-100 Toruń, Poland

(Received September 11, 1998)

In this communication we present results of measurements of low temperature thermoluminescence, isothermal decays, steady state radioluminescence yield, and scintillation time profiles at various temperatures on two scintillator materials, BaF_2:Ce and undoped BaF_2. We find that all these results can be consistently interpreted in the frame of a model that includes several relatively shallow charge traps. We have identified and characterized one particular shallow trap that causes the decay of the dominant scintillation component of BaF_2:Ce to be slower than radiative, as well as a set of others that are responsible for even slower components in the scintillation time profile of this material.

PACS numbers: 78.60.Kn, 78.60.Ya, 78.55.Hx, 29.40.Mc

Thermoluminescence provides a useful tool for studying host-to-ion energy transfer and the role of traps in scintillator materials. While it is generally accepted that deep traps, revealed by high-temperature thermoluminescence (htTL, 300 K and higher) can reduce the scintillation light yield of any scintillator material [1, 2], the importance of shallower traps has only recently been recognized [3–5]. Although their glow peaks fall at temperatures well below ambient, such shallower traps can introduce slow components in both the rising and decaying parts of the scintillation time profiles and reduce the scintillation light yield at room temperature (RT). Specific examples of these effects have recently been identified in LuAP:Ce ($LuAlO_3$:Ce) and YAP:Ce ($YAlO_3$:Ce) [4, 5]. In this communication we report results of studies on BaF_2:Ce, a promising scintillator material [6] as well

*The results of this paper were initially presented at *The Jabłoński Centennial Conference on Luminescence and Photophysics, July 23–27, 1998, Toruń, Poland.*

†e-mail: jglodo@phys.uni.torun.pl; fax: 48-56-6225397

as on undoped BaF_2. These studies include low-temperature thermoluminescence (ltTL, below 300 K), isothermal phosphorescence decays (ITD), steady state radioluminescence (SSR) and scintillation time profiles (STP) at various temperatures. The results of all experiments are interpreted in the frame of a simple model based on first-order kinetics.

In Fig. 1 we present room temperature time profiles of BaF_2:0.2 mol% Ce under optical (*a*) and gamma (*b*) excitations measured at a wavelength of 323 nm. The optical excitation was provided by monochromatized synchrotron emission tuned to the Ce^{3+} $f-d$ absorption band at 200 nm, delivered in 1.5 ns pulses 180 ns apart. The decay of the resulting Ce-emission was almost exactly single-exponential with a dominant component of 31 ns, characteristic of the Ce^{3+} $d-f$ transition in BaF_2. Under γ-excitation from a Ru^{106} radioactive source, however, the scintillation decay was more complex. On a time scale of 400 ns a two-exponential fit yielded two components of 47 ns and 280 ns, with contributions of 72% and 23%, respectively. Similar results for the same concentration of cerium were reported by Visser et al. [6]. Comparison between optical and scintillation time profiles indicates that, as in LuAP:Ce and YAP:Ce [3–5], traps are involved in the process of energy transfer from the host to the Ce-ions and that trap lifetimes at RT must be on the order of a few tens to hundreds of nanoseconds.

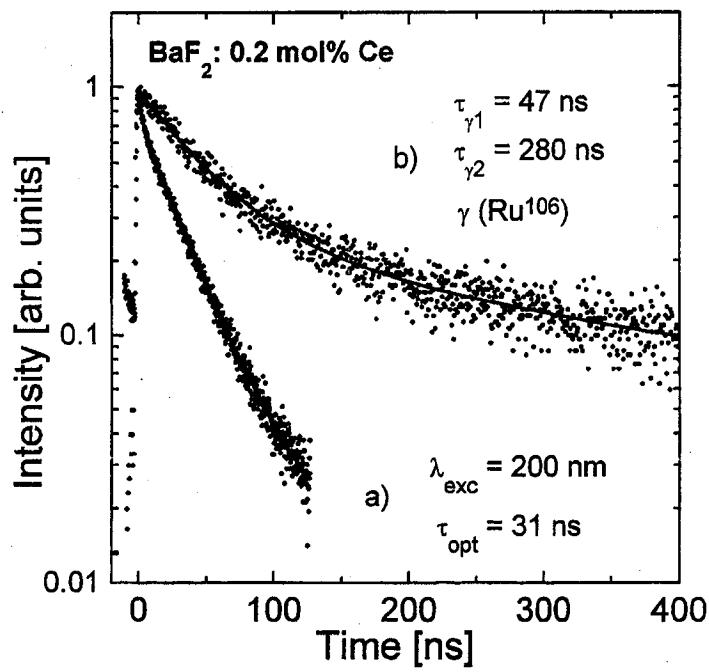

Fig. 1. Room temperature scintillation and photoluminescence time profiles of BaF_2:Ce. Filled circles represent experimental points; solid lines show two-exponential fits to measured points (see Table I).

The ltTL glow curves of Ce-doped and undoped BaF_2 crystals measured at a heating rate of 9 K/min are shown by experimental points (filled circles) in Fig. 2. Prior to TL runs the samples were irradiated for 20 hours by an X-ray source (Am^{241}) at 4 K. The undoped crystal exhibits three well developed glow peaks at 109 K (labeled #1), 223 K (#2), and 270 K. The Ce-doped crystal glow curve is more complex, with three clearly visible peaks at 109 K (labeled *a*), 159 K (*b*), and 225 K (*c*), and at least two additional weaker peaks at about 135 K (β) and 170 K (γ). In general agreement with other experiments, both earlier [7] and recent [8], we note that certain peaks (1 and *a*, 2 and *c*), present in both undoped and Ce-doped crystals, are most likely due to dissociation or thermal annealing of intrinsic defects such as V_k centers, while the remaining peaks are due to other processes involving defects induced by Ce-doping. For simplicity we will use the conventional term "traps" to cover all these cases, bearing in mind that the reality is far more complex.

Also plotted in Fig. 2 is a set of simulated glow curves, each corresponding to a different characteristic trap. These are depicted by solid lines, except for one (designated α) that corresponds to a hypothetical trap identified by the decay

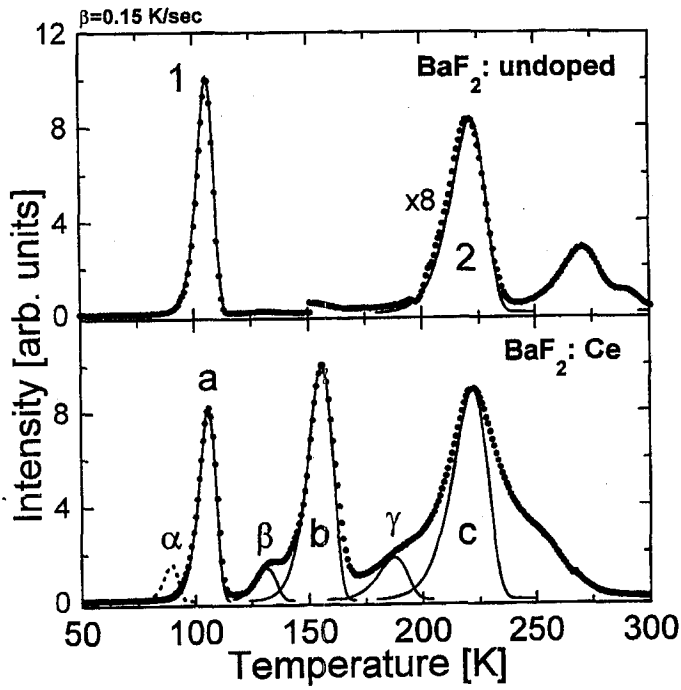

Fig. 2. Thermoluminescence glow curves of BaF_2 and BaF_2:Ce following X-ray irradiation at 4 K. Filled circles represent experimental points; solid and dashed lines represent calculated curves with parameters derived from a different experiment (see the text). With the exception of shifts to correct for thermal lag (3 K for BaF_2:Ce, 2.4 K for BaF_2), there is no other adjustable parameter. Heating rate was 9 K/min.

traces alone. Calculations were performed separately for each of the glow peaks according to the Randall and Wilkins formula for first-order kinetics [9]:

$$I(T) = n_0 s \exp\left(-\frac{E}{k_B T}\right) \exp\left[-\frac{s}{\beta}\int_{T_0}^{T} \exp\left(-\frac{E}{k_B T}\right) \mathrm{d}T\right], \tag{1}$$

where T is the sample temperature, n_0 the initial filled trap concentration, s the frequency factor, k_B the Boltzmann constant, E the trap depth defined by the activation energy, and β the heating rate. The procedure by which the values of parameters E and s have been established for all traps, including α, will be outlined below.

In Fig. 3 we show the SSR intensity as a function of temperature. In this experiment the sample was continuously excited by γ-rays coming from a Cs^{137} radioactive source and the total light emitted by the sample collected and measured by a photomultiplier tube (PMT). To avoid any interference from TL the temperature ramp was negative, beginning at RT and reduced in steps down to 4 K. At each step the specimen was allowed about ten minutes for temperature equilibration, after which the instantaneous intensity was determined by recording

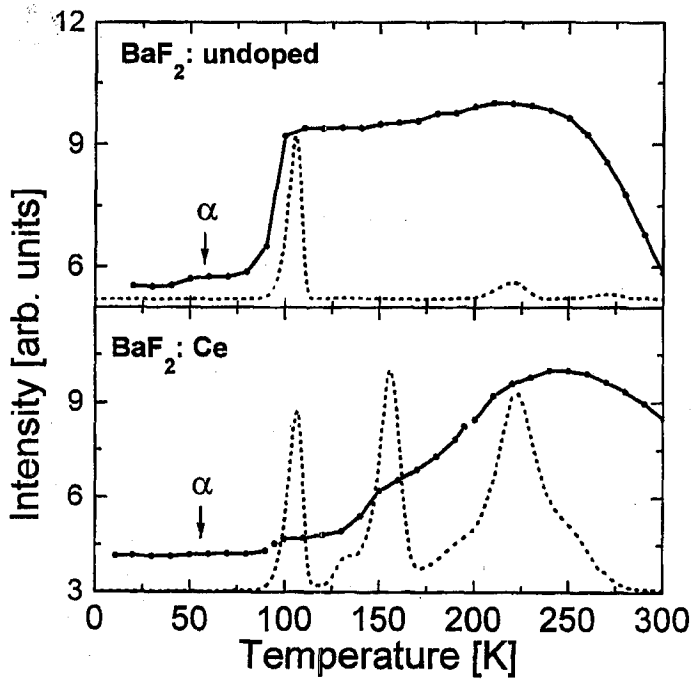

Fig. 3. Steady state radioluminescence intensity of BaF_2 and BaF_2:Ce as a function of temperature. Experimental points are shown by filled circles joined by a solid line. Dashed lines show measured thermoluminescence glow curves for comparison. An arrow indicates predicted position of glow peak of a hypothetical trap α in BaF_2 and BaF_2:Ce (see the text).

and averaging 500 sampling points over a period of about five minutes. Although more detailed quantitative interpretation of these results for BaF_2 and BaF_2:Ce must await later publication, we note here a definite correspondence between the temperatures of the glow peaks in the TL curves and the locations of a step-like structure in the SSR curves. This is not surprising, since the increase in trap lifetimes as the temperature drops means that the carriers are retained longer, more effectively preventing them from recombining and contributing to the emission. Consequently (at least until the traps are filled), the steady state emission intensity should be lower at lower temperatures. Also note the more gradual drop of SSR intensity from 250 to 100 K in BaF_2:Ce compared to undoped BaF_2, most likely due to the presence of additional traps in the cerium-doped material. The undoped material also shows a very small but distinct step at about 50 K, which we attribute to the previously mentioned hypothetical trap α, whose glow peak is not measured.

In Fig. 4 we show STP of BaF_2:Ce, measured at selected temperatures to illustrate some general trends. At the lowest temperature (20 K) the profile is almost entirely composed of the single prompt component characteristic of the Ce radiative lifetime of 31 ns; any carriers that entered traps are essentially retained

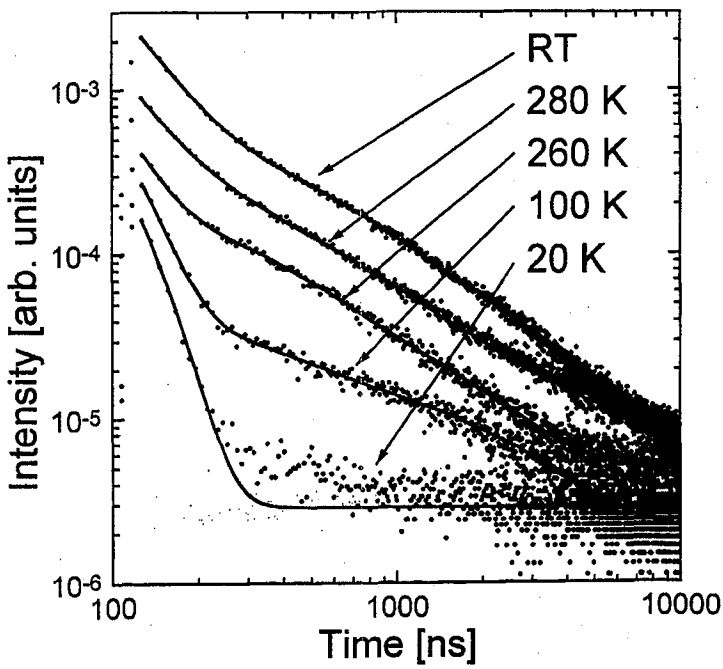

Fig. 4. Scintillation time profiles of BaF_2:Ce for various temperatures. Experimental points are shown by filled circles, solid lines represent three- or four-exponential fits to points (see the text). Both axes are presented on logarithmic scales to maximize their range.

indefinitely, and cannot contribute to the emission kinetics. This component must, of course, be present at the higher temperatures as well, but, as is evident from the traces, is gradually overwhelmed by the contributions from slower components generated by carriers liberated from deeper and deeper traps. In Table I we summarize results of three- and four-exponential fits to all the profiles measured. For some profiles the fitting procedure was performed with the decay time of the first component held fixed at 31 ns.

TABLE I

Summary of results of time profile measurements and fits for BaF_2:Ce. Decay times and normalized zero-time amplitudes represent parameters derived from the multi-exponential fits. The figure in which a particular profile is identified, along with the excitation mode (optical into $f-d$ Ce^{3+} absorption or gamma) and the temperature of the measurement. The asterisk (*) indicates that a given value was held fixed.

Figs.	Exc.	Temp. [K]	y_0 [%]	A_1 [%]	τ_1 [ns]	A_2 [%]	τ_2 [ns]	A_3 [%]	τ_3 [ns]	A_4 [%]	τ_4 [ns]
1	200 nm	RT	1.5	75.5	31.1	23	2.8	–	–	–	–
	γ	RT	4.7	72.5	47	22.8	280	–	–	–	–
4&5	γ	20	1.8	98.2	30.3	–	–	–	–	–	–
		100	0.8	85.8	32.8	7.4	339	6	1963	–	–
		150	1.2	75.3	33.4	13.3	223	10.2	1345	–	–
		200	0.7	54.2	31*	27.3	66	12.6	392	5.2	2435
		250	1.4	61.7	33	24.1	369	12.8	1276	–	–
		260	1.2	57.1	32.3	30.2	267	11.5	1230	–	–
		280	0.8	39	31*	35.3	90	20.4	456	4.5	2670
		RT	0.4	29.5	31*	45.7	67	18.4	378	6	1840
		320	0.4	33.7	31*	41.6	63.7	19.7	331	4.6	1352

Complementary information is provided by the measurement of ITD, whose results are summarized in Table II. In this experiment the sample was irradiated at 4 K to attain a high population of occupied traps. Then, unlike the TL measurements, the temperature of the sample was raised *quickly* to some predetermined higher value and *held there* for an appropriate time (up to 2700 s) while the decay of the emission released from the sample was recorded against time. These decays are due to radiative recombination that follows thermally activated release of carriers from traps, allowing direct measurement of the effective trap lifetimes at those temperatures.

In order to extract the energy depth of the trap from its lifetime, we utilize the relationship:

$$\tau = s^{-1} \exp\left(\frac{E}{k_B T}\right), \tag{2}$$

TABLE II

Summary of results of ITD measurements for BaF_2 and BaF_2:Ce. Decay times and normalized zero-time amplitudes represent parameters derived from the multiexponential fits, along with the time scale of the measurement. The asterisk (*) indicates that a given value was held fixed.

Crystal	Temp. [K]	y_0 [%]	A_1 [%]	τ_1 [s]	A_2 [%]	τ_2 [s]	A_3 [%]	τ_3 [s]	Scale [s]
	100	0*	100	214	–	–	–	–	2600
	104	0*	100	60	–	–	–	–	1600
BaF_2	120	66.7	10.6	23.8	22.7	350	–	–	1800
	215	0.9	24.6	22.8	49.1	107	25.4	328	1900
	220	3.3	43.7	30.5	53	131	–	–	1700
	100	0*	100	144	–	–	–	–	2000
	104	0*	100	51.3	–	–	–	–	1400
	109	1	98	13.6	1	635	–	–	700
	130	11.5	71.1	25.6	17.4	183	–	–	400
	136	0*	52.9	31	23.7	122	23.4	2505	900
BaF_2:Ce	151	1	38.8	25.3	52.1	79.4	8.1	285	2100
	155	1.3	74.4	26.2	24.3	113	–	–	600
	159	1.1	94.2	31	4.7	280	–	–	1200
	180	9	65.5	48	25.5	512	–	–	2700
	210	1.8	50.7	35.6	36.8	122	10.7	515	1550
	220	1.8	80.9	45	13.8	223	3.5	938	2400
	225	11.1	39.4	180	49.5	902	–	–	1600

or, equivalently,

$$\ln \tau = \frac{E}{k_B} T^{-1} - \ln s. \tag{3}$$

In principle, this should be all we need, and if we were dealing with only a single trap we could plot $\ln \tau$ vs. T^{-1} and solve for energy depth E and frequency factor s uniquely. Unfortunately, however, we are dealing not with a single trap but a small ensemble of them, and must settle for something less than uniqueness. Nevertheless, we can save the day by assuming that all the traps have essentially the same frequency factor s. Then, by taking the log of Eq. (3)

$$\ln(\ln \tau + \ln s) = \ln(T^{-1}) + \ln\left(\frac{E}{k_B}\right), \tag{4}$$

and making a different plot, shown in Fig. 5, we obtain a set of parallel lines whose vertical shifts are determined solely by trap depths E. In this figure the experimental points come from both ITD and STP experiments on BaF_2 and BaF_2:Ce. It is of more than passing interest that while the experimental points

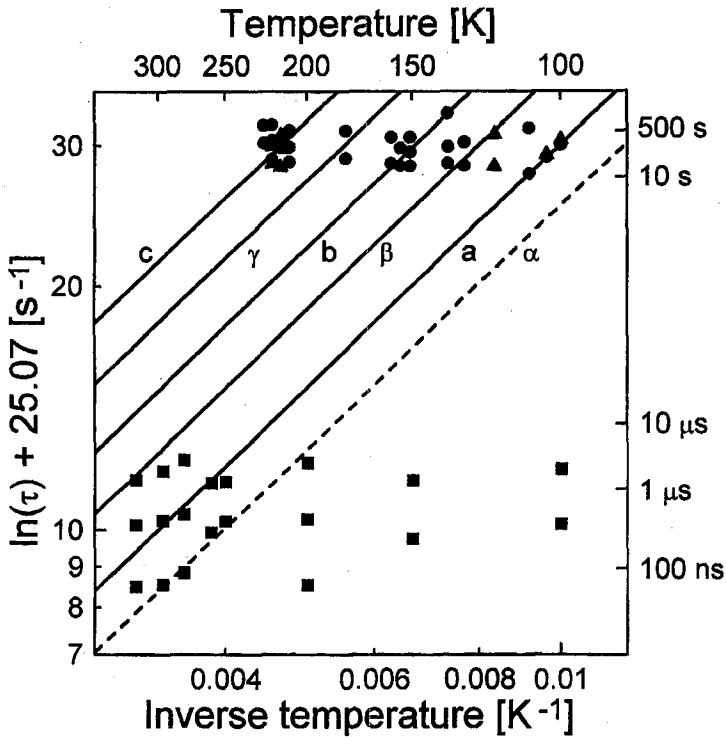

Fig. 5. Trap lifetimes as function of temperature. Points in the diagram were obtained from fits to decays measured in two different experiments, ITD and STP, at various temperatures. The ITD points of BaF_2 are shown by triangles, those of BaF_2:Ce by circles, and the STP points of BaF_2:Ce by squares. The value for ln s of 25.07, assumed common to all traps, was derived from a standard Arrhenius fit of the data for trap a, the only one for which precise points could be obtained from both ITD and STP measurements. The other solid lines (traps present in TL) and the dashed line (trap found in STP) were drawn parallel to the one from trap a, with their vertical positions (corresponding to trap depths) defined by fits to the relevant points. Both axes are presented on logarithmic scales; note that the experimental points span nearly 10 orders of magnitude in time. The expression for the y variable was derived from Eq. (4).

span a range of about ten orders of magnitude, sets of them can be identified that clearly belong to the same straight line (or the trap it represents), which we designate as a. This enables us to use Eq. (3) to find the appropriate value of ln$s$ to be 25.07, defining the common frequency factor for all the traps as 7.7×10^{10} s^{-1}. The energy depth of this particular trap a was found from the same fit to be 0.259 eV.

To verify these results we used them to calculate theoretical glow curves which we compared to experimental ltTL points. The position of the calculated curve failed to coincide with the corresponding measured one by only 3 K (for BaF_2:Ce) and 2.4 K (for BaF_2), which we attribute to a thermal lag between the

measured and the true sample temperatures. After correcting for this effect we obtained the curves shown by solid lines in Fig. 2 to correspond to the two glow peaks designated a and 1. Since the simulated curves were calculated without recourse to the experimental TL data, the agreement speaks for itself.

Emboldened by these results, we found energy depths for all the other traps for which we were able to identify straight lines in Fig. 5, labeled b, c, β, and γ. Using these values we calculated the simulated glow curves shown in Fig. 2. Except for the shifts to correct for thermal lag (2.4 K for BaF_2, 3 K for BaF_2:Ce), which were applied to all the peaks calculated for the respective materials, no other adjustable parameter was used. In all cases the agreement between experimental and simulated glow peaks is remarkably good.

The straight line a in Fig. 5 is the line corresponding to the shallowest trap for which there are points from both ITD and STP experiments. There are, however, STP points below this line that clearly belong to another parallel and straight line, designated α. This line must be related to an even shallower trap, but no corresponding ltTL glow peak has been found. We can speculate on possible reasons, such as a relatively low concentration of the relevant defect and/or a relatively small energy barrier for detrapping carriers preventing it from retaining an adequate number of carriers, but can offer no definitive explanation. Other traps (β and γ), identified with the help of a diagram shown in Fig. 5, produce much weaker glow peaks which nevertheless are clearly identifiable in the ltTL glow curves of Fig. 2. Note also the spread of ITD points at line c; this spread, apparently wider for BaF_2:Ce than for undoped BaF_2, correlates well with the structure shown by the peak c.

The parameters of all the traps established with the help of the procedures described above are summarized in Table III. In this table we also show the room

TABLE III

Summary of trap parameters obtained from the fits shown in Fig. 5. The trap lifetimes given in the table were calculated at 297 K. The same frequency factor, $s = 7.72 \times 10^{10}$ s^{-1}, obtained from the fit to STP and ITD points assigned to the trap a, has been assumed for all the traps.

Crystal	Trap	E [eV]	τ [ns]
	α	0.217	62.3
	a	0.259	322
BaF_2:Ce	β	0.323	3.9×10^3
	b	0.385	44.2×10^3
	γ	0.467	1.1×10^6
	c	0.555	34×10^6
BaF_2	1	0.259	322
	2	0.555	34×10^6

temperature lifetimes of all the traps. It is interesting to note that the lifetimes of the two shallowest traps, α and a, explain the shape of the scintillation time profile in BaF_2:Ce. The combined effect of the two contributions of 31 and 62.3 ns, due to "direct" and shallow trap-mediated processes, respectively, produce a decay that has an effective fast component of about 50 ns, as shown in Fig. 1b. A range of deeper traps, listed in Table III, contribute to even slower components.

The presence of STP points below the line α suggest the presence of even shallower traps. However, more experiments are clearly needed to find definitive evidence of their existence. We plan to extend our experiments to include even shorter times, in the hope of providing more data in the region of the diagram below the α line.

The results presented in this communication indicate that traps actively participate in the scintillation process in BaF_2:Ce. In particular traps are responsible for the slower than radiative decay of the fast scintillation component and for a significant loss of the light yield at room temperature by diversion into a range of slower components. Improvement of the material requires that traps be removed or that their concentrations be strongly reduced. Since some of these traps are presumably of intrinsic nature, the improvements may prove hard to achieve.

This work was supported by the U.S. Department of Energy (grant No. DE-FG02-96-ER82117 and DE-FG-02-90-ER61033), by the Committee for Scientific Research (Poland), grant No. 2P03B04914, and by ALEM Associates, Boston. We are also grateful to Dr. J. Sutherland and his group at the U11 beamline at NSLS, Brookhaven National Lab., Upton, NY for their assistance in VUV experiments. The continuous support of Profs. A. Lempicki and C. Brecher of Boston University is also gratefully acknowledged.

References

[1] K. Meijvogel, A.J.J. Bos, P. Dorenbos, C.W.E. van Eijk, in: *Proc. Int. Conf. on Inorganic Scintillators and Their Applications, SCINT95, Delft 1995*, Eds. P. Dorenbos, C.W.E. van Eijk, Delft University Press, Delft 1996, p. 159.

[2] R.H. Bartram, D.S. Hamilton, L.A. Kappers, A. Lempicki, *J. Lumin.* **75**, 183 (1997).

[3] A.J. Wojtowicz, W. Drozdowski, D. Wisniewski, K.R. Przegietka, H.L. Oczkowski, T.M. Piters, *Rad. Meas.* **29**, 323 (1998).

[4] A.J. Wojtowicz, J. Glodo, W. Drozdowski, K.R. Przegietka, *J. Lumin.* **79**, 275 (1998).

[5] A.J. Wojtowicz, J. Glodo, A. Lempicki, C. Brecher, *J. Phys., Condens. Matter* **10**, 8401 (1998).

[6] R. Visser, P. Dorenbos, C.W.E. van Eijk, R.W. Hollander, P. Schotanus, *IEEE Trans. Nucl. Sci.* **38**, 178 (1991).

[7] W. Hayes, *Crystals with the Fluorite Structure*, Clarendon Press, Oxford 1974.

[8] B. Yang, P.D. Townsend, A.P. Rowlands, *Phys. Rev. B* **57**, 178 (1998).

[9] J.T. Randall, M.H.F. Wilkins, *Proc. R. Soc. Lond. A* **184**, 366 (1945).